NONLINEAR CONTROL OF A DOUBLY FED INDUCTION GENERATOR SUPPLIED BY A MATRIX CONVERTER FOR WIND ENERGY CONVERSION SYSTEMS

Zinelaabidine. BOUDJEMA **Abdelkader. MEROUFEL**
Intelligent Control and Electrical Power Systems Laboratory, University of Sidi Bel-abbes, Algeria.
boudjemaa1983@yahoo.fr ameroufel@yahoo.fr

Elhadj. BOUNADJA **Youcef. DJERRIRI**
University of Chlef – Algeria. University of Sidi Bel-abbes, Algeria.
e.bounadja@univ-chlef.dz djeriri_youcef@yahoo.fr

Abstract: *This paper deals with a variable speed device to produce electrical energy on a power network, based on a doubly-fed induction generator fed by a matrix converter. In the first place, we carried out a study of modelling on the matrix converter controlled by the venturini modulation technique. In second place, we developed a model of the doubly fed induction generator. In order to control the power flowing between the stator of the DFIG and the power network, a control law is synthesized using two types of controllers: fuzzy logic and sliding mode. Their respective performances are compared in terms of power reference tracking, response to sudden speed variations, sensitivity to perturbations and robustness against machine parameters variations.*

Key words: *Doubly fed induction generator, matrix converter, fuzzy logic controller, sliding mode controller.*

1. Introduction

Wind energy is the most promising renewable source of electrical power generation for the future. Many countries promote the wind power technology through various national programs and market incentives. Wind energy technology has evolved rapidly over the past three decades with increasing rotor diameters and the use of sophisticated power electronics to allow operation at variable speed [1]. Doubly fed induction generator is one of the most popular variable speed wind turbines in use nowadays. It is normally fed by a voltage source inverter. However, currently the three phase matrix converters have received considerable attention because they may become a good alternative to voltage-source inverter pulse width-modulation topology. This is because the matrix converter provides bi-directional power flow, nearly sinusoidal input/output waveforms, and a controllable input power factor. Furthermore, the matrix converter allows a compact design due to the lack of dc-link capacitors for energy storage. Consequently, in this work, a three-phase matrix converter is used to drive the doubly fed induction generator.

A lot of works have been presented with diverse control diagrams of DFIG. These control diagrams are usually based on vector control notion with conventional PI controllers as proposed by Pena et al. in [2]. The similar conventional controllers are also used to realize control techniques of DFIG when grid faults appear like unbalanced voltages [3,4] and voltage dips [5]. It has also been shown in [6,7] that glimmer problems could be resolved with suitable control strategies. Many of these works prove that stator reactive power control can be an adapted solution to these diverse problems.

This paper discusses the control of electrical power exchanged between the stator of the DFIG and the power network by controlling independently the active and reactive power. After modeling the DFIG and choosing the appropriate *d-q* reference frame, active and reactive powers are controlled using two types of nonlinear controllers: fuzzy logic and sliding mode. The two controllers are compared in terms of power reference tracking, sensitivity to perturbations and robustness against machine parameters variations.

2. Matrix converter modeling

The matrix converter performs the power conversion directly from AC to AC without any intermediate dc link. It is very simple in structure and has powerful controllability. The converter consists of a matrix of bi-directional switches linking two independent three-phase systems. Each output line is linked to each input line via a bi-directional switch. Figure 1 shows the basic diagram of a matrix converter.

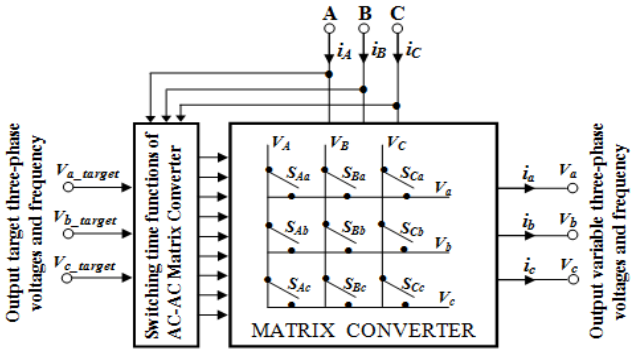

Fig. 1. Schematic representation of the matrix converter.

The switching function of a switch S_{mn} in figure 1 is given by :

$$S_{mn} = \begin{cases} 1 & S_{mn} \text{ closed} \\ 0 & S_{mn} \text{ open} \end{cases} \quad m \in \{A,B,C\},\ n \in \{a,b,c\} \tag{1}$$

The mathematical expression that represents the operation of the matrix converter in figure 1 can be written as :

$$\begin{bmatrix} V_a \\ V_b \\ V_c \end{bmatrix} = \begin{bmatrix} S_{Aa} & S_{Ab} & S_{Ac} \\ S_{Ba} & S_{Bb} & S_{Bc} \\ S_{Ca} & S_{Cb} & S_{Cc} \end{bmatrix} \cdot \begin{bmatrix} V_A \\ V_B \\ V_C \end{bmatrix} \tag{2}$$

$$\begin{bmatrix} i_A \\ i_B \\ i_C \end{bmatrix} = \begin{bmatrix} S_{Aa} & S_{Ba} & S_{Ca} \\ S_{Ab} & S_{Bb} & S_{Cb} \\ S_{Ac} & S_{Bc} & S_{Cc} \end{bmatrix}^T \cdot \begin{bmatrix} i_a \\ i_b \\ i_c \end{bmatrix} \tag{3}$$

To determine the behavior of the matrix converter at output frequencies well below the switching frequency, a modulation duty cycle can be defined for each switch.

The input/output relationships of voltages and currents are related to the states of the nine switches and can be expressed as follows :

$$\begin{bmatrix} V_a \\ V_b \\ V_c \end{bmatrix} = \begin{bmatrix} k_{Aa} & k_{Ab} & k_{Ac} \\ k_{Ba} & k_{Bb} & k_{Bc} \\ k_{Ca} & k_{Cb} & k_{Cc} \end{bmatrix} \cdot \begin{bmatrix} V_A \\ V_B \\ V_C \end{bmatrix} \tag{4}$$

$$\begin{bmatrix} i_A \\ i_B \\ i_C \end{bmatrix} = \begin{bmatrix} k_{Aa} & k_{Ba} & k_{Ca} \\ k_{Ab} & k_{Bb} & k_{Cb} \\ k_{Ac} & k_{Bc} & k_{Cc} \end{bmatrix}^T \cdot \begin{bmatrix} i_a \\ i_b \\ i_c \end{bmatrix} \tag{5}$$

With :

$$0 \le k_{mn} \le 1, \quad m = A, B, C, \quad n = a, b, c \tag{6}$$

The variables k_{mn} are the duty cycles of the nine switches S_{mn} and can be represented by the duty-cycle matrix k. In order to prevent a short circuit on the input side and ensure uninterrupted load current flow, these duty cycles must satisfy the three following constraint conditions :

$$k_{Aa} + k_{Ab} + k_{Ac} = 1 \tag{7}$$
$$k_{Ba} + k_{Bb} + k_{Bc} = 1 \tag{8}$$
$$k_{Ca} + k_{Cb} + k_{Cc} = 1 \tag{9}$$

The high-frequency synthesis technique introduced by Venturini (1980) and Alesina and Venturini (1988), allows a control of the S_{mn} switches so that the low frequency parts of the synthesized output voltages (V_a, V_b and V_c) and the input currents (i_A, i_B and i_C) are purely sinusoidal with the prescribed values of the output frequency, the input frequency, the displacement factor and the input amplitude.

Where θ is the initial phase angle. The output voltage is given by :

$$\begin{bmatrix} V_a \\ V_b \\ V_c \end{bmatrix} = \begin{bmatrix} 1+2\delta\cos\alpha & 1+2\delta\cos(\alpha-\frac{2\pi}{3}) & 1+2\delta\cos(\alpha-\frac{4\pi}{3}) \\ 1+2\delta\cos(\alpha-\frac{4\pi}{3}) & 1+2\delta\cos\alpha & 1+2\delta\cos(\alpha-\frac{2\pi}{3}) \\ 1+2\delta\cos(\alpha-\frac{2\pi}{3}) & 1+2\delta\cos(\alpha-\frac{4\pi}{3}) & 1+2\delta\cos\alpha \end{bmatrix} \cdot \begin{bmatrix} V_A \\ V_B \\ V_C \end{bmatrix} \tag{10}$$

Where : $\begin{cases} \alpha = \omega_m + \theta \\ \omega_m = \omega_{output} - \omega_{input} \end{cases}$

The running matrix converter with Venturini algorithm generates at the output a three-phases sinusoidal voltages system having in that order pulsation ω_m, a phase angle θ and amplitude $\delta.V_s$ ($0 < \delta < 0.866$ with modulation of the neural) [8].

3. Doubly fed induction generator modeling

For a doubly fed induction machine, the Concordia and Park transformation's application to the traditional *a*, *b*, *c* model allows to write a dynamic model in a *d-q* reference frame as follows:

$$\begin{cases} V_{ds} = R_s I_{ds} + \frac{d}{dt}\psi_{ds} - \omega_s \psi_{qs} \\ V_{qs} = R_s I_{qs} + \frac{d}{dt}\psi_{qs} + \omega_s \psi_{ds} \\ V_{dr} = R_r I_{dr} + \frac{d}{dt}\psi_{dr} - \omega_r \psi_{qr} \\ V_{qr} = R_r I_{qr} + \frac{d}{dt}\psi_{qr} + \omega_r \psi_{dr} \end{cases}, \begin{cases} \psi_{ds} = L_s I_{ds} + M I_{dr} \\ \psi_{qs} = L_s I_{qs} + M I_{qr} \\ \psi_{dr} = L_r I_{dr} + M I_{ds} \\ \psi_{qr} = L_r I_{qr} + M I_{qs} \end{cases} \tag{11}$$

The stator and rotor angular velocities are linked by the following relation : $\omega_s = \omega + \omega_r$.

This electrical model is completed by the mechanical equation :

$$C_{em} = C_r + J\frac{d\Omega}{dt} + f\Omega \tag{12}$$

Where the electromagnetic torque C_{em} can be written as a function of stator fluxes and rotor currents :

$$C_{em} = pp\frac{M}{L_s}(\psi_{qs} I_{dr} - \psi_{ds} I_{qr}) \tag{13}$$

In order to easily control the production of electricity by the wind turbine, we will carry out an independent control of active and reactive powers by orientation of the stator flux.

By choosing a reference frame linked to the stator flux, rotor currents will be related directly to the stator active and reactive power. An adapted control of these currents will thus permit to control the power exchanged between the stator and the grid. If the stator flux is linked to the d-axis of the frame we have :

$$\psi_{ds} = \psi_s \quad \text{and} \quad \psi_{qs} = 0 \tag{14}$$

and the electromagnetic torque can then be expressed as follows :

$$C_{em} = -pp\frac{M}{L_s} I_{qr}\psi_{ds} \tag{15}$$

By substituting Eq.15 in Eq.12, the following rotor flux equations are obtained :

$$\begin{cases} \psi_s = L_s I_{ds} + M I_{dr} \\ 0 = L_s I_{qs} + M I_{qr} \end{cases} \tag{16}$$

In addition, the stator voltage equations are reduced to :

$$\begin{cases} V_{ds} = R_s I_{ds} + \dfrac{d}{dt}\psi_s \\ V_{qs} = R_s I_{qs} + \omega_s \psi_s \end{cases} \tag{17}$$

By supposing that the electrical supply network is stable, having for simple voltage V_s, that led to a stator flux ψ_s constant. This consideration associated with Eq.16 shows that the electromagnetic torque only depends on the q-axis rotor current component. With these assumptions, the new stator voltage expressions can be written as follows :

$$\begin{cases} V_{ds} = R_s I_{ds} \\ V_{qs} = R_s I_{qs} + \omega_s \psi_s \end{cases} \tag{18}$$

Using Eq.17, a relation between the stator and rotor currents can be established :

$$\begin{cases} I_{ds} = -\dfrac{M}{L_s} I_{dr} + \dfrac{\psi_s}{L_s} \\ I_{qs} = -\dfrac{M}{L_s} I_{qr} \end{cases} \tag{19}$$

The stator active and reactive powers are written :

$$\begin{cases} P_s = V_{ds} I_{ds} + V_{qs} I_{qs} \\ Q_s = V_{qs} I_{ds} - V_{ds} I_{qs} \end{cases} \tag{20}$$

By using Eqs.11, 12, 19 and 20, the statoric active and reactive power, the rotoric fluxes and voltages can be written versus rotoric currents as :

$$\begin{cases} P_s = \dfrac{\omega_s \psi_s M}{L_s} I_{qr} \\ Q_s = -\dfrac{\omega_s \psi_s M}{L_s} I_{dr} + \dfrac{\omega_s {\psi_s}^2}{L_s} \end{cases} \tag{21}$$

$$\begin{cases} \psi_{dr} = (L_r - \dfrac{M^2}{L_s}) I_{dr} + \dfrac{M\psi_s}{L_s} \\ \psi_{qr} = (L_r - \dfrac{M^2}{L_s}) I_{qr} \end{cases} \tag{22}$$

$$\begin{cases} V_{dr} = R_r I_{dr} + (L_r - \dfrac{M^2}{L_s})\dfrac{dI_{dr}}{dt} - g\omega_s (L_r - \dfrac{M^2}{L_s}) I_{qr} \\ V_{qr} = R_r I_{qr} + (L_r - \dfrac{M^2}{L_s})\dfrac{dI_{qr}}{dt} + g\omega_s (L_r - \dfrac{M^2}{L_s}) I_{dr} + g\omega_s \dfrac{M\psi_s}{L_s} \end{cases} \tag{23}$$

In steady state, the second derivative terms of the two equations in 24 are nil. We can thus write :

$$\begin{cases} V_{dr} = R_r I_{dr} - g\omega_s (L_r - \dfrac{M^2}{L_s}) I_{qr} \\ V_{qr} = R_r I_{qr} + g\omega_s (L_r - \dfrac{M^2}{L_s}) I_{dr} + g\omega_s \dfrac{M\psi_s}{L_s} \end{cases} \tag{24}$$

The third term, which constitutes cross-coupling terms, can be neglected because of their small influence. These terms can be compensated by an adequate synthesis of the regulators in the control loops.

4. Controllers synthesis

In this section, we have chosen to compare the performances of the DFIG with two different nonlinear controllers: fuzzy logic and sliding mode.

A. Fuzzy logic controller (FLC)

When the conventional controllers, such as the Proportional Integral (PI) does not allow to obtain extremely high performances and that we do not have an important computing power to establish a standard predictive regulation, the fuzzy logic control proves to be an interesting approach. This type of control, approaching the human reasoning that makes use of the tolerance, uncertainty, imprecision and fuzziness in the decision-making process, manages to offer a very satisfactory performance, without the need of a detailed mathematical model of the system just by incorporating the experts' knowledge into fuzzy rules. In addition, it has inherent abilities to deal with imprecise or noisy data; thus, it is able to extend its control capability even to those operating conditions where linear control techniques fail (i.e., large parameter variations).

The main preference of the fuzzy logic is that is easy to implement control that it has the ability of generalization. The approach of the basic structure of the fuzzy logic controller system is illustrated in figure 2 [9].

Input and output are non-fuzzy values and the basic configuration of the fuzzy logic controller (FLC) is featured in figure 3.

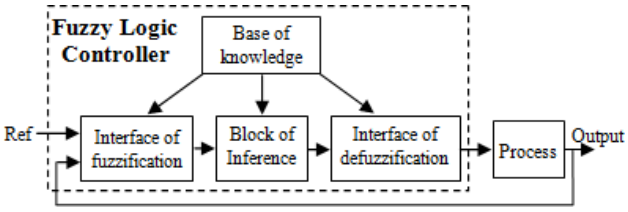

Fig. 2. Structure of fuzzy logic controller.

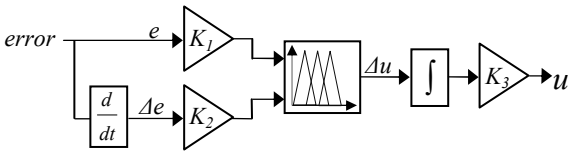

Fig. 3. Block diagram of fuzzy logic controller.

In the system presented in this study, Mamdani type of fuzzy logic is used for the powers and currents controllers [10]. The input signals are the powers and currents errors ($e_P(k)$, $e_Q(k)$, $e_{Idr}(k)$ and $e_{Iqr}(k)$) and their change rate ($\Delta e_P(k)$, $\Delta e_Q(k)$, $\Delta e_{Idr}(k)$ and $\Delta e_{Iqr}(k)$). The powers and currents errors are respectively calculate with comparison between their references ($P_{s\text{-}ref}$, $Q_{s\text{-}ref}$, $I_{dr\text{-}ref}$ and $I_{qr\text{-}ref}$) and their measured values ($P_{S\text{-}mes}$, $Q_{S\text{-}mes}$, I_{dr} and I_{qr}).

As it's shown by figure 2, fuzzy logic controller is based on three well known blocs: Fuzzyfication bloc, block of rule bases and defuzzyfication block, whose function is following briefly explained. The fuzzyfication stage transforms crisp values from a process into fuzzy sets. The second stage is the fuzzy rule bases which expresses relations between the input fuzzy sets of linguistic description rules A, B and the output fuzzy set C in the form of "IF A and B–THEN", and the defuzzyfication stage transforms the fuzzy sets in the output space into crisp control signals.

For the four fuzzy logic controllers proposed, the universes of discourses are first partitioned into the seven linguistic variables NB, NM, NS, EZ, PP, PM, PG, triangular membership functions are chosen to represent the linguistic variables and fuzzy singletons for the outputs are used. The fuzzy rules that produce these control actions are reported in table 1.

We use the following designations for membership functions:

- NB: Negative Big,
- NM: Negative Middle,
- NS: Negative Small,
- EZ: Equal Zero,
- PS: Positive Small,
- PM: Positive Middle,
- PB: Positive Big.

Table 1 : Matrix of inference.

ΔE \ E	NB	NM	NS	EZ	PS	PM	PB
NB	NB	NB	NB	NB	NM	NS	EZ
NM	NB	NB	NB	NM	NS	EZ	PS
NS	NB	NB	NM	NS	EZ	PS	PM
EZ	NB	NM	NS	EZ	PS	PM	PB
PS	NM	NS	EZ	PS	PM	PB	PB
PM	NS	EZ	PS	PM	PB	PB	PB
PB	EZ	PS	PM	PB	PB	PB	PB

These choices are described in figure 4.

B. Sliding mode controller (SMC)

The sliding mode technique is developed from variable structure control to solve the disadvantages of other designs of nonlinear control systems. The sliding mode is a technique to adjust feedback by previously defining a surface. The system which is controlled will be forced to that surface, then the behavior of the system slides to the desired equilibrium point.

The main feature of this control is that we only need to drive the error to a "switching surface". When the system is in "sliding mode", the system behavior is not affected by any modeling uncertainties and/or disturbances. The design of the control system will be

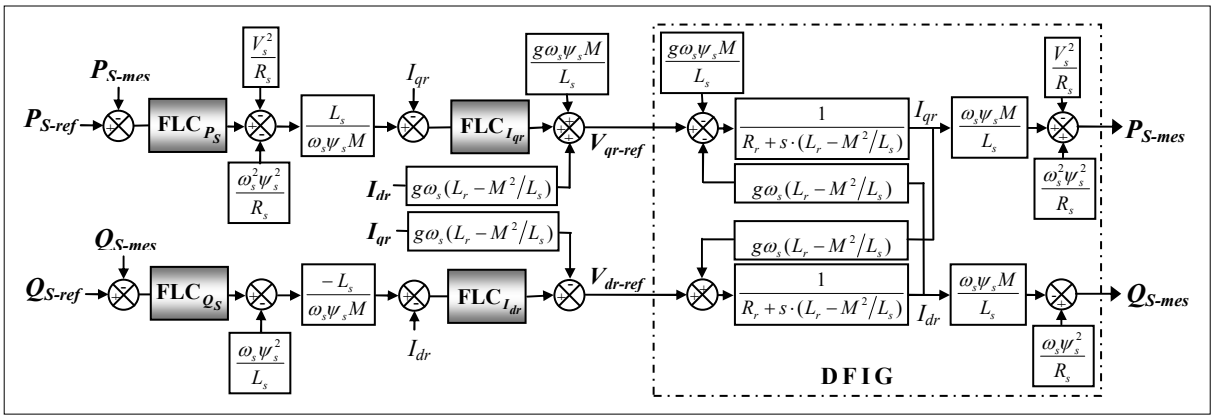

Fig. 4. Structure of fuzzy logic controller.

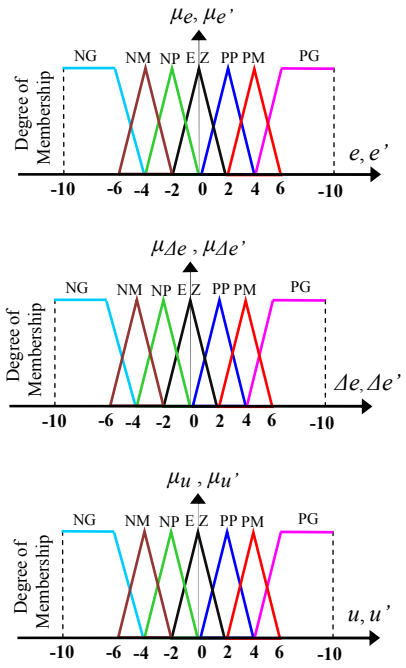

Fig. 5. Fuzzy sets and its memberships functions.

demonstrated for a nonlinear system presented in the canonical form [11] :

$$\dot{x} = f(x,t)+B(x,t)U(x,t),\ x\in R^n,\ U\in R^m,\ ran(B(x,t)) = m \tag{25}$$

with control in the sliding mode, the goal is to keep the system motion on the manifold S, which is defined as :

$$S = \{x : e(x, t)=0\} \tag{26}$$

$$e = x^d - x \tag{27}$$

Here e is the tracking error vector, x^d is the desired state, x is the state vector. The control input U has to guarantee that the motion of the system described in (25) is restricted to belong to the manifold S in the state space. The sliding mode control should be chosen such that the candidate Lyapunov function satisfies the Lyapunov stability criteria:

$$\vartheta = \frac{1}{2}S(x)^2, \tag{28}$$

$$\dot{\vartheta} = S(x)\dot{S}(x). \tag{29}$$

This can be assured for :

$$\dot{\vartheta} = -\eta|S(x)| \tag{30}$$

Here η is strictly positive. Essentially, equation (28) states that the squared "distance" to the surface, measured by $e(x)^2$, decreases along all system trajectories. Therefore (29), (30) satisfy the Lyapunov condition. With selected Lyapunov function the stability of the whole control system is guaranteed. The control function will satisfy reaching conditions in the following form :

$$U^{com} = U^{eq} + U^n \tag{31}$$

Here U^{com} is the control vector, U^{eq} is the equivalent control vector, U^n is the correction factor and must be calculated so that the stability conditions for the selected control are satisfied.

$$U^n = K\ \text{sat}((S(x)/\delta) \tag{32}$$

sat$((S(x)/\delta)$ is the proposed saturation function, δ is the boundary layer thickness. In this paper we propose the Slotine method :

$$S(X) = \left(\frac{d}{dt} + \lambda\right)^{n-1} e \tag{33}$$

Here, e is the tracking error vector, λ is a positive coefficient and n is the relative degree.

In our study, we choose the error between the measured and references stator powers as sliding mode surfaces, so we can write the following expression:

$$\begin{cases} S_d = P_{S-ref} - P_S \\ S_q = Q_{S-ref} - Q_S \end{cases} \tag{34}$$

The first order derivate of (34), gives :

$$\begin{cases} \dot{S}_d = \dot{P}_{S-ref} - \dot{P}_S \\ \dot{S}_q = \dot{Q}_{S-ref} - \dot{Q}_S \end{cases} \tag{35}$$

Replacing the powers in (35) by their expressions given in (21), one obtains:

$$\begin{cases} \dot{S}_1 = \dot{P}_{S-ref} - \dfrac{\omega_s\psi_s M}{L_s}\dot{I}_{qr} \\ \dot{S}_2 = \dot{Q}_{S-ref} + \dfrac{\omega_s\psi_s M}{L_s}\dot{I}_{dr} - \dfrac{\omega_s{\psi_s}^2}{L_s} \end{cases} \tag{36}$$

V_{dr} and V_{qr} will be the two components of the control vector used to constraint the system to converge to S_{dq}=0. The control vector V_{dqeq} is obtained by imposing $\dot{S}_{dq} = 0$ so the equivalent control components are given by the following relation :

$$V_{eqdq} = \begin{bmatrix} -\dfrac{L_s\left(L_r - \dfrac{M^2}{L_s}\right)}{\omega_s\psi_s M}\dot{Q}_s^* + R_r I_{dr} - \left(L_r - \dfrac{M^2}{L_s}\right)g\omega_s I_{qr} + \dfrac{\left(L_r - \dfrac{M^2}{L_s}\right)\psi_s}{M} \\ \dfrac{L_s}{\omega_s\psi_s M}\dot{P}_s^* + R_r I_{qr} - \left(L_r - \dfrac{M^2}{L_s}\right)g\omega_s I_{dr} + \dfrac{g\omega_s\psi_s M}{L_s} \end{bmatrix} \tag{37}$$

To obtain good performances, dynamic and commutations around the surfaces, the control vector is imposed as follows :

$$V_{dq} = V_{eqdq} + \mathrm{K}\cdot sat\,(S_{dq}) \tag{38}$$

The sliding mode will exist only if the following condition is met :

$$S \cdot \dot{S} < 0 \qquad (39)$$

5. Simulation results and discussions

In this section, simulations are realized with a 1.5 MW generator coupled to a 398V/50Hz grid. The machine's parameters are given next in appendix. In the objective to evaluate the performances of the controllers, three categories of tests have been realized: pursuit test, sensitivity to the speed variation and robustness facing variations of the machine's parameters.

A. Pursuit test

This test has for goal the study of the two controllers behaviours in reference tracking, while the machine's speed is considered constant at its nominal value. The simulation results are presented in figure 6. As it's shown by this figure, for the two controllers, the active and reactive generated powers tracks almost perfectly their references. In addition and contrary to the FLC controller where the coupling effect between the two axes is very clear, we can notice that the SMC controller ensures a perfect decoupling between them. Therefore we can consider that the sliding mode controller has a very good performance for this test.

B. Sensitivity to the speed variation

The aim of this test is to analyze the influence of a speed variation of the DFIG on active and reactive powers. For this objective and at time = 0.015s, the speed was varied from 150 rad/s to 100 rad/s. The simulation results are shown in figure 7. This figure express that the speed variation produced an important osciallions on the powers curves of the system with FLC controller, while the effect is almost negligible for the system with SMC one. We can notice that this last has a nearly perfect speed disturbance rejection, indeed; only very small power variations can be observed (fewer than 3%). This result is attractive for wind energy applications to ensure stability and quality of the generated power when the speed is varying.

C. Robustness

In order to test the robustness of the used controllers, the machines' parameters have been intentionally modified with overkill variations: the values of the stator and the rotor resistances R_s and R_r are doubled and the values of inductances L_s, L_r and M are divided by 2. The machine is running at its nominal speed. The gotten results are represented on figure 8.

These results show that parameters variations of the DFIG presents a clear effect on the powers curves and that the effect proves more significant for FLC controller than that with SMC one. This result enables us to conclude that this last controller is more robust.

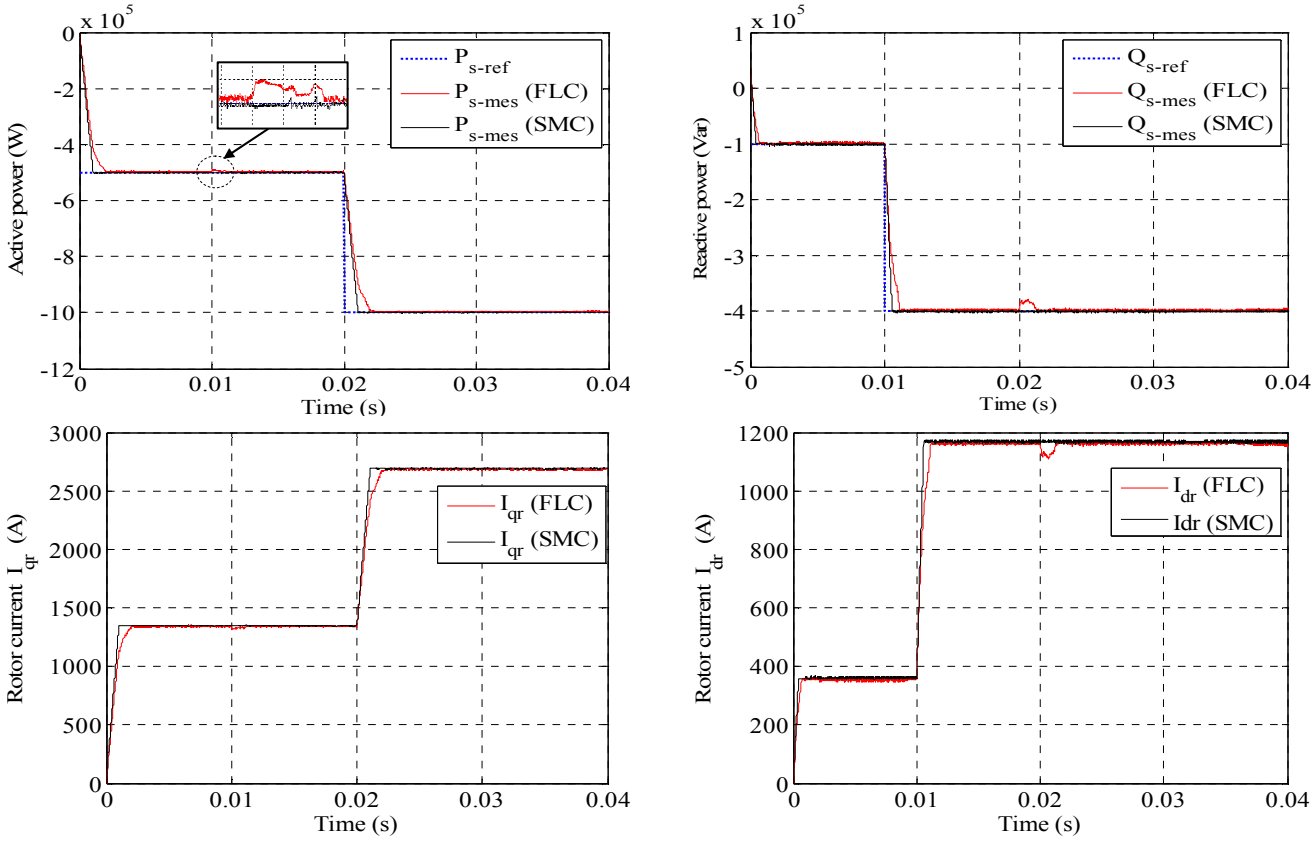

Fig. 6. Reference tracking.

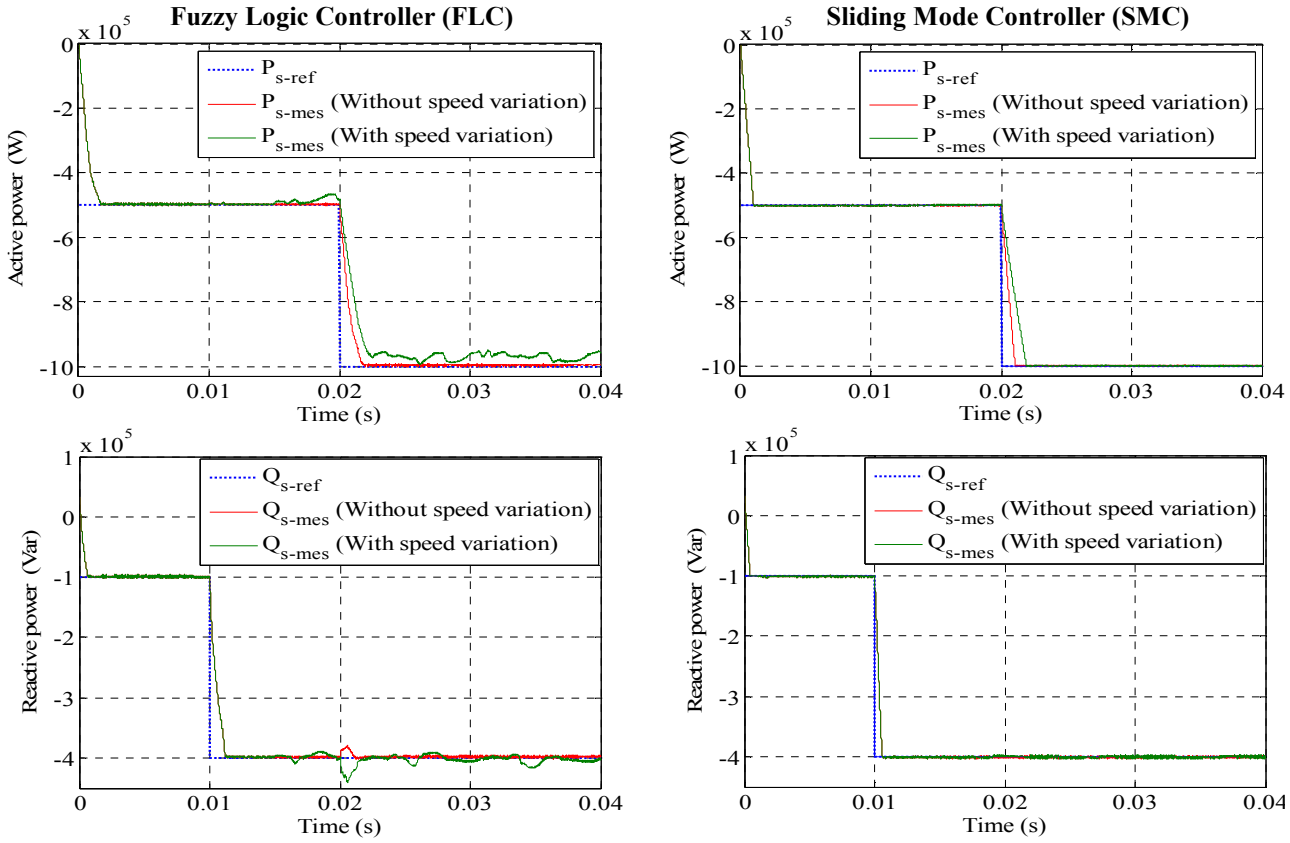

Fig. 7. Sensitivity to the speed variation.

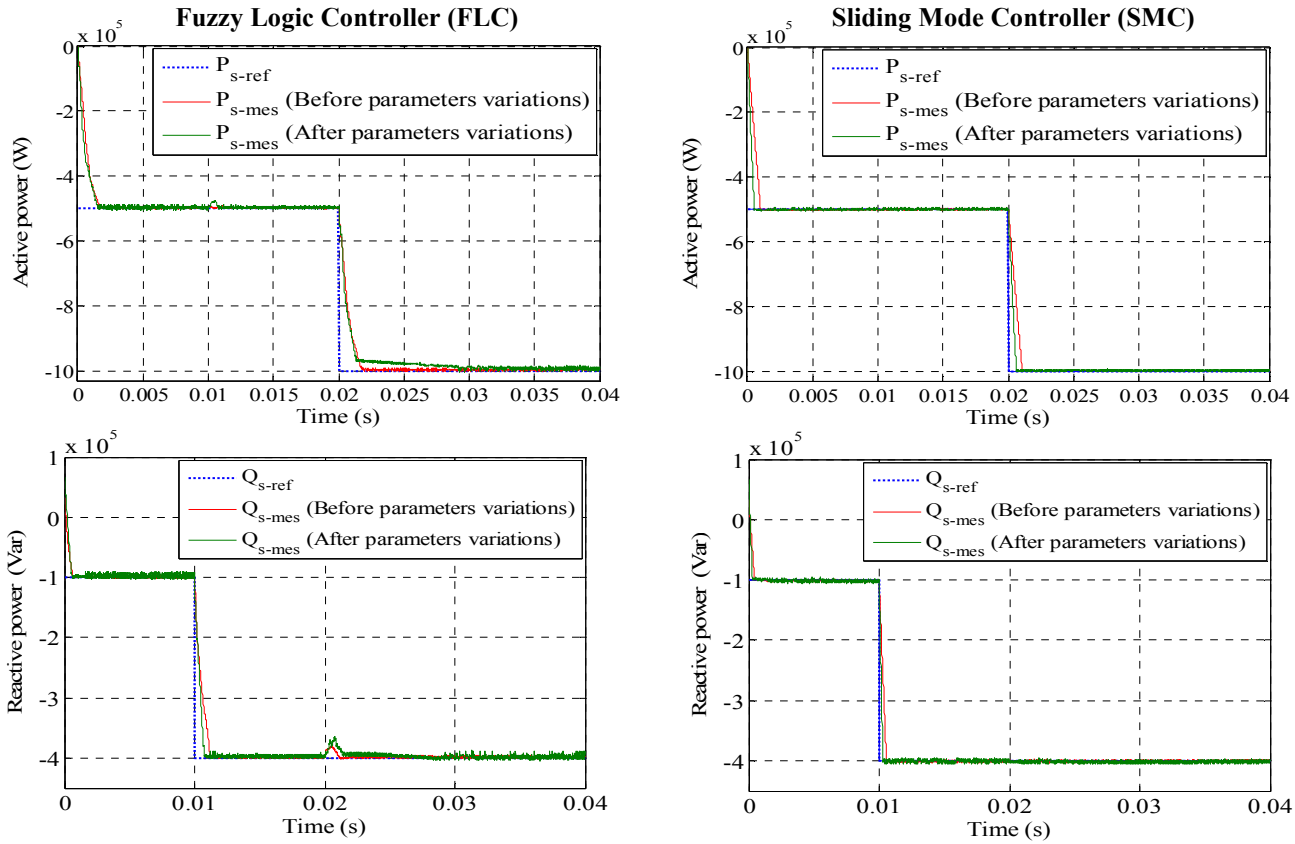

Fig. 8. Sensitivity to the machine's parameters variation on the DFIG control.

6. Conclusion

The modeling, the control and the simulation of an electrical power electromechanical conversion system based on a doubly fed induction generator (DFIG) connected directly to the grid by the stator and fed by a matrix converter on the rotor side has been presented in this study. Our objective was the implementation of a robust decoupled control system of active and reactive powers generated by the stator side of the DFIG, in order to ensure of the high performance and a better execution of the DFIG, and to make the system insensible with the external disturbances and the parametric variations. In the first step, we started with a study of modeling on the matrix converter controlled by the Venturini modulation technique, because this later present a reduced harmonic rate and the possibility of operation of the converter at the input unit power factor. In second step, we adopted a vector control strategy in order to control statoric active and reactive power exchanged between the DFIG and the grid. In third step, two different controllers are synthesized and compared. In term of power reference tracking with the DFIG in ideal conditions, the SMC ensures a perfect decoupling between the two axes comparatively to the FLC where the coupling effect between them is very clear. When the machine's speed is modified, the impact on the active and reactive powers values is important for FLC controller whereas it is almost negligible for SMC one. A robustness test has also been investigated where the machine's parameters have been modified. These changes induce some disturbances on the powers responses but with an effect almost doubled with the FLC controller than on that with SMC one. Basing on all these results we conclude that robust control method as SMC can be a very attractive solution for devices using DFIG such as wind energy conversion systems.

Appendix

Table 2. Machine parameters.

Parameters	Rated Value	Unity
Nominal power	1.5	MW
Stator voltage	398	V
Stator frequency	50	Hz
Number of pairs poles	2	
Nominal speed	150	rad/s
Stator resistance	0.012	Ω
Rotor resistance	0.021	Ω
Stator inductance	0.0137	H
Rotor inductance	0.0136	H
Mutual inductance	0.0135	H

References

1. Anaya-Lara, O., Jenkins, N., Ekanayake, J., Cartwright, P., Hughes, M.: *Wind Energy Generation*. In : Wiley, (2009).
2. Pena, R., Clare, J. C., Asher, G. M.: *A doubly fed induction generator using back to back converters supplying an isolated load from a variable speed wind turbine*. In: IEE Proceeding on Electrical Power Applications 143 (September (5)) 1996.
3. Poller, M. A.: *Doubly-fed induction machine models for stability assessment of wind farms*. In: Power Tech Conference Proceedings, 2003, IEEE, Bologna, vol. 3, 23–26 June 2003.
4. Brekken, T., Mohan, N.: *A novel doubly-fed induction wind generator control scheme for reactive power control and torque pulsation compensation under unbalanced grid voltage conditions*. In: IEEE 34th Annual Power Electronics Specialist Conference, 2003, PESC'03, 15-19 June 2003, vol. 2, pp. 760-764.
5. Brekken, T. K. A., Mohan, N.: *Control of a doubly fed induction wind generator under unbalanced grid voltage conditions*. In: IEEE Transaction on Energy Conversion, 22 (March (1)) 2007 129–135.
6. Lopez, J., Sanchis, P., Roboam, X., Marroyo, L.: *Dynamic behavior of the doubly fed induction generator during three-phase voltage dips*. In: IEEE Transaction on Energy Conversion, 22 (September (3)) 2007, 709–717.
7. Sun, T., Chen, Z., Blaabjerg, F.: *Flicker study on variable speed wind turbines with doubly fed induction generators*. IEEE Transactions on Energy Conversion, 20 (December (4)), 2005, 896–905.
8. Venturini M., *A new sine wave in sine wave out conversion technique which eliminates reactive elements*, In: Proc Powercon 7, San Diego, CA, pp E3-1, E3-15, 27-24 March 1980.
9. Chaiba, A., Abdessemed, R., Bendaas, M. L., Dendouga, A.: *Performances of Torque Tracking Control for Doubly Fed Asynchronous Motor using PI and Fuzzy Logic Controllers*. Journal of Electrical Engineering, Vol.5, N°2, pp. 25-30, Romania, 2005.
10. Mamdani, E. H., and Assilian, S.: *An experiment in linguistic synthesis with a fuzzy logic controller*. International Journal of Machine Studies. Vol. VII, pp.1-13, 1975.
11. Yan, Z., Jin, C., Utkin, V. I.: *Sensorless Sliding-Mode Control of Induction Motors*, IEEE Trans. Ind. electronic. 47 No. 6 (December 2000), 1286–1297.